

Theory for the excitation spectrum of High- T_c superconductors : quasiparticle dispersion and shadows of the Fermi surface

M. Langer, J. Schmalian, S. Grabowski, and K. H. Bennemann

Institut für Theoretische Physik, Freie Universität Berlin, Arnimallee 14, 14195 Berlin, Germany
(15 may 1995)

Using a new method for the solution of the FLEX-equations, which allows the determination of the self energy $\Sigma_{\mathbf{k}}(\omega)$ of the 2D Hubbard model on the real frequency axis, we calculate the doping dependence of the quasi-particle excitations of High- T_c superconductors. We obtain new results for the shadows of the Fermi surface, their dependence on the deformation of the quasi particle dispersion, an anomalous ω -dependence of $\text{Im}\Sigma_{\mathbf{k}}(\omega)$ and a related violation of the Luttinger theorem. This sheds new light on the influence of short range magnetic order on the low energy excitations and its significance for photoemission experiments.

74.25.Jb,79.60.-i,71.27.+a

Despite an enormous progress [1], the electronic excitation spectrum of the strongly correlated High- T_c superconductors is still far from being understood. Recent angular resolved photoemission measurements [2–6] for different doping concentrations demonstrate that pronounced deformations of the quasiparticle dispersion occur. The opening of a spin density gap and the variation in spectral weight as function of \mathbf{k} [6] reflect the strong influence of the antiferromagnetic correlations on the low energy excitations. In particular, the interpretation of the shadows of the Fermi surface (FS) observed by Aebi *et al.* [4] in terms of antiferromagnetic correlations is under current debate [7]. Therefore, the determination of the elementary excitations with high energy and momentum resolution is of extreme importance.

In this Letter, we calculate the quasiparticle excitation spectrum of the one band Hubbard Hamiltonian using a new numerical method for the self consistent summation of all bubble and ladder diagrams [8] (fluctuation exchange approximation) on the real frequency axis, and compare our results with recent photoemission experiments. Due to the high degree of numerical stability of this method, we present interesting new results for a strong deformation of the quasiparticle dispersion at the wave vector $\mathbf{k} = (\pi, 0)$ upon doping, the occurrence of satellite peaks and shadows of the Fermi surface in the paramagnetic state and an unusual momentum and frequency dependence of the electronic self energy. All this sheds new light on the occurrence of FS-shadows without long range antiferromagnetic order.

The fluctuation exchange (FLEX) approximation [8–11] is conserving in the sense of Kadanoff and Baym [12]. It is a theoretical approach complementary to the exact diagonalization studies [13] or quantum Monte Carlo simulations [14,15], which gave deep insight into the origin of the quasiparticles of strongly correlated systems, but are limited to rather small systems. The self energy in the FLEX approximation of the paramagnetic phase is given by the momentum and

Matsubara-frequency sum $\Sigma(k) = \frac{T}{N} \sum_{k'} V(k-k')G(k')$, where $k = (\mathbf{k}, i\omega_n)$. The effective interaction $V(q)$ results from the summation of bubble and ladder diagrams and can be expressed in terms of the particle-hole bubble $\chi(q) = -\frac{T}{N} \sum_k G(k+q)G(k)$. [8] $G(k)$ is the fully renormalized Greens function, ω_n a fermionic Matsubara frequency, \mathbf{k} the crystal momentum, N the number of lattice sites, and T the temperature.

Because of the straightforward applicability of the numerically very effective fast Fourier transformation (FFT) for the evaluation of the above convolutions, most of the solutions of the FLEX equations are performed on the imaginary frequency axis. Unfortunately, from the imaginary axis, reliable information about the real frequency excitations can only be obtained using rather ill defined numerical procedures. Based on the contour integral technique, we present in the following a numerically stable calculation of the electronic self energy on the real axis using the FFT. Note that recently Dahm *et al.* [11] also solved the FLEX equations on the real axis. However, they performed the direct calculation of the rather time consuming frequency integrals.

In the following, we first apply our approach to the one band Hubbard model in the paramagnetic state. The bare dispersion is given by $\varepsilon_{\mathbf{k}}^o = -2t_o(\cos(k_x) + \cos(k_y)) - \mu$, with nearest neighbor hopping element $t_o = 0.25$ eV, and chemical potential μ . The local Coulomb repulsion is given by $U = 4t_o$. The extension to multi band Hamiltonians and to superconducting or magnetic phases is straightforward. [16] We solve the set of equations for complex frequencies $z = \omega + i\gamma$ with small but finite imaginary part $\gamma < \pi T$. Then, the analytical continuation to the real axis $\gamma \rightarrow 0^+$ is numerically well defined.

The above momentum summations become simple products in Wannier space. Furthermore, the frequency summations are evaluated using the contour integral technique [17], where we place the four horizontal lines of the contour by a finite amount γ away from the poles of the Greens function. Considering the particle hole bub-

ble $\chi_{\mathbf{i}}(z)$ at lattice site \mathbf{i} and for frequencies $z = \omega + i\gamma$, we perform the Kramers Kronig transformation for the Greens function and express the resulting energy denominators using Laplace transformation [18]. Now, the occurring frequency integrals decouple and we obtain $\chi_{\mathbf{i}}(z) = \int_0^\infty dt \chi_{\mathbf{i}}(t) e^{izt}$ with

$$\chi_{\mathbf{i}}(t) = -i(2\pi)^2 e^{-\gamma t} (\varrho_{\mathbf{i}}(t)[\mathcal{A}_{-\mathbf{i}}^*(t) + \mathcal{A}_{-\mathbf{i}}(-t)e^{2\gamma t}] - \varrho_{-\mathbf{i}}^*(t)[\mathcal{A}_{\mathbf{i}}(t) + \mathcal{A}_{\mathbf{i}}^*(-t)e^{2\gamma t}]) . \quad (1)$$

Here, $\mathcal{A}_{\mathbf{i}}(t)$ is defined by

$$\mathcal{A}_{\mathbf{i}}(t) = \frac{i}{2\pi} \int_{-\infty}^{\infty} \frac{d\epsilon}{2\pi} f^*(\epsilon + i\gamma) G_{\mathbf{i}}^*(\epsilon + i\gamma) e^{-i\epsilon t} , \quad (2)$$

and $\varrho_{\mathbf{i}}(t)$ is the Fourier transform of the spectral density $-\frac{1}{\pi} \text{Im} G_{\mathbf{i}}(\epsilon + i\gamma)$. Note that we are using the complex Fermi function $f(z)$, because we solve the FLEX equations consistently for finite γ . This is essential for the fine structure at small energies. Thus $\chi_{\mathbf{k}}(z)$ and finally $V_{\mathbf{k}}(z)$ can be evaluated by a $D + 1$ dimensional FFT of $\chi_{\mathbf{i}}(t)$. The procedure for the frequency summation of the self energy is similar. Within the Wannier space, it follows for the Laplace transform of the self energy:

$$\Sigma_{\mathbf{i}}(t) = -i2\pi T V_{\mathbf{i}}(0) \varrho_{\mathbf{i}}(t) + i(2\pi)^2 e^{-\gamma t} (v_{\mathbf{i}}(t)[\mathcal{A}_{\mathbf{i}}(t) + \mathcal{A}_{\mathbf{i}}^*(-t)e^{2\gamma t}] - \varrho_{\mathbf{i}}(t)[\mathcal{B}_{\mathbf{i}}^*(t) + \mathcal{B}_{\mathbf{i}}(-t)e^{2\gamma t}]) . \quad (3)$$

$v_{\mathbf{i}}(t)$ is the Fourier transform of $-\frac{1}{\pi} \text{Im} V_{\mathbf{i}}(z)$ and $\mathcal{B}_{\mathbf{i}}(t)$ can be obtained from Eq. 2 by replacing $f^*(z)G_{\mathbf{i}}^*(z)$ by $n^*(z)V_{\mathbf{i}}^*(z)$. $n(z)$ is the complex Bose function, and the first term results from the coincidence of the fermionic Matsubara frequencies $\omega_n = \omega_{n'}$, which cannot be included in the standard contour. Thus, the self energy $\Sigma_{\mathbf{k}}(\omega + i\gamma)$ results via $D + 1$ dimensional FFT [19] from $\Sigma_{\mathbf{i}}(t)$ and the limit $\gamma \rightarrow 0^+$ can be performed.

The advantage of our method compared to the first real frequency calculation recently published by Dahm *et al.* [11] is the applicability of the FFT and the consistent solution for a small but finite imaginary part γ , which lead to an accuracy of the convergence of the spectral density per momentum and frequency point of 10^{-5} . Only this accuracy enables us to obtain the new physical results presented here [20].

In the inset of Fig. 1, we show results for the local (momentum averaged) density of states (DOS) for various doping values. We find for larger doping a rigid band like behavior, but for smaller doping a pseudogap occurs as a precursor of the Mott-Hubbard splitting. From the asymmetry with respect to the pseudogap, a transfer of spectral weight from high energy to low energy scales [21] can be seen.

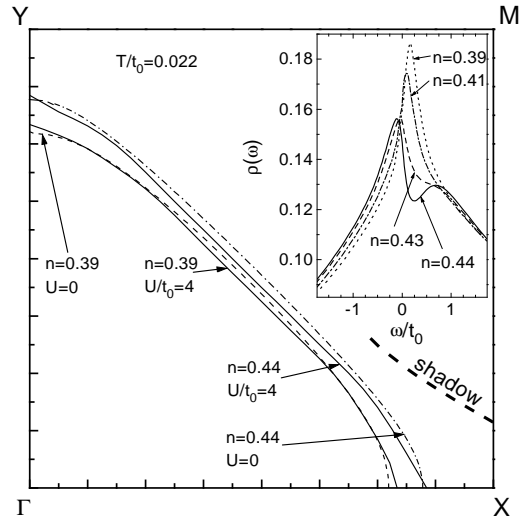


FIG. 1. Fermi surface in the quarter of the Brillouin zone with $k_x, k_y > 0$ (solid line) in comparison with the Fermi surface of the uncorrelated system for different doping concentrations. Note the violation of the Luttinger theorem and the occurrence of FS-shadows for smaller doping ($n = 0.44$). The inset shows the local density of states for various doping values. Note, the occurrence of a pseudogap near the half filled case.

In Fig. 1, results are shown for the FS for different band fillings in comparison with that for $U = 0$. The FS is obtained from the \mathbf{k} -points, where $\epsilon_{\mathbf{k}}^0 + \text{Re}\Sigma_{\mathbf{k}}(0) = 0$. The changes of the FS are rather small, but a tendency to a stronger nesting topology is clearly visible. Such a deformation of the FS is related to a dramatic deformation of the quasi particle dispersion. For larger doping, the Luttinger theorem [22] is fulfilled. However, for smaller doping the volume of the FS decreases compared to the $U = 0$ case. This violation of the Luttinger theorem results from a transfer of particles to additional shadow states (schematically shown in Fig. 1), as will be discussed below.

In Fig. 2, we show our results for the quasi particle dispersion obtained from the maxima of the spectral density. Since we expect the FLEX to be a good approximation for the low energy excitations, we focus on the dispersion near the Fermi energy and in particular in the neighborhood of the X-point. For larger doping (dashed line), the saddle point, responsible for the van Hove singularity, is visible. However, for smaller doping (solid and open-crossed squares) pronounced deformations of the dispersion occur. The dispersion of the states with high spectral weight (solid squares) is flattened and suddenly repelled from the Fermi energy. This might be a precursor of the large spin density gap at the X-point, found in

recent photoemission experiments by Wells *et al.* [6] for undoped cuprates. Furthermore, new quasiparticle states with low spectral weight (open-crossed squares) occur. These states, which are for larger doping only visible far away from the Fermi level (not shown), remain stable for low excitation energies and build up the shadows of the Fermi surface [4], which one usually would expect only for systems with long range antiferromagnetic order. In order to check this interpretation, we performed for the first time the spin resolved FLEX approximation within a given antiferromagnetic background (solid line). We fixed the staggered moment m_s by its Hartree Fock value, because for the doping values under consideration no long range order occurs. The dispersion in this antiferromagnetic background is a clear continuation of the evolution of the paramagnetic state with decreasing doping. Obviously, a clear precursor of the antiferromagnetic state occurs already in the paramagnetic phase without broken symmetry.

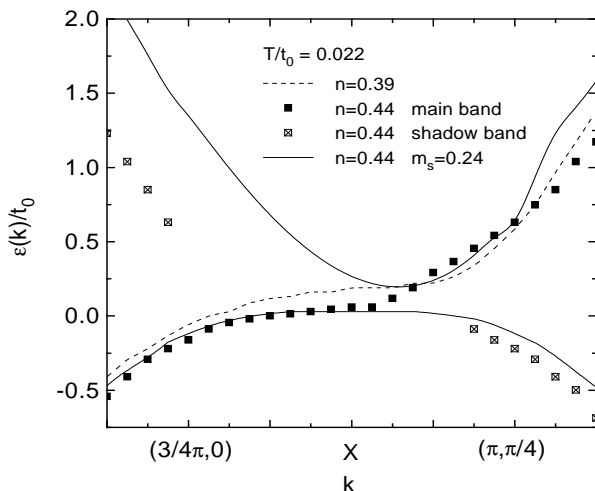


FIG. 2. Quasiparticle dispersion in the neighborhood of the X -point for different doping concentrations. Note that for smaller doping ($n = 0.44$) two bands exist near the Fermi energy in the paramagnetic state. The dispersion of the main band (solid squares) resembles that of the highly doped system (dashed line). Considering both, the main band and the shadow band (open-crossed squares) one recognizes the evolution towards the two branches of the dispersion in an antiferromagnetic background (solid lines).

In Fig. 3, we show the occurrence of shadows of the FS by plotting the spectral density $\rho_{\mathbf{k}}(\omega)$ for \mathbf{k} -points between the X and M -point. Besides the main peak, not crossing the FS, satellite peaks near the Fermi energy can clearly be observed. These satellite peaks are the new quasi particle states of Fig. 2 (open-crossed squares), which build up the shadows of the FS. For the wave

vector $\mathbf{k} = (\pi, \pi/8)$, which is shifted by (π, π) with respect to the main FS, the shadow band crosses the Fermi level. The intensity of the shadow states (ca. 10% of the main peak) agrees with the experimental observation [4]. The possible occurrence of such shadow states for a system without long range antiferromagnetic order was originally proposed by Kampf and Schrieffer [23]. Using a phenomenological ansatz for the spin susceptibility, they argued that for sufficient long ranged antiferromagnetic correlations a coupling of states \mathbf{k} and \mathbf{k}' with $|\mathbf{k}' - \mathbf{k} - \mathbf{Q}| < \xi^{-1}$ might lead to distinct shadow states. From their calculation one can estimate the magnetic correlation length ξ to be of the order of 20 lattice spacings, to obtain observable satellite peaks. This is much larger than the correlation length observed in neutron scattering experiments [24], which is only a few lattice spacings.

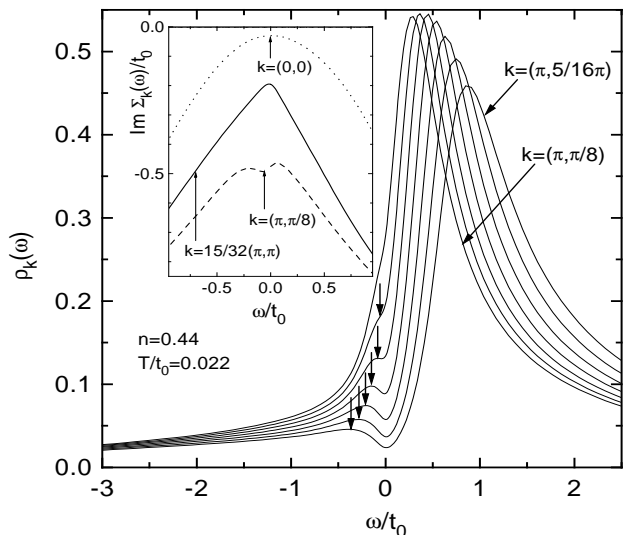


FIG. 3. Spectral density for \mathbf{k} -points between the X and M -point, i.e. $\mathbf{k} = (\pi, \frac{l}{32}\pi)$ with $l = 4 \dots 10$. The main peak reflects the dispersion of the bands similar to the case for $U = 0$. The satellites, indicated by the arrows, build up the shadows of the Fermi surface. The inset shows the imaginary part of the self energy for different momenta.

Therefore, it was argued in Ref. [7] that there cannot be a well defined kinematics of the antiferromagnetic spin excitations that lead to the observations of Aebi *et al.* [4]. However, in our calculation the correlation length, obtained from the \mathbf{k} -dependence of $V_{\mathbf{k}}(\omega)$, is 2.5 lattice spacings, in agreement with those experiments. Furthermore, we find that for larger doping ($n = 0.4$) the shadow states at low energies vanish, although the correlation length only decreases slightly. In order to resolve a shadow peak at $\mathbf{k}' = \mathbf{k} + \mathbf{Q}$, the excitation energies of the states near \mathbf{k} should be within an energy range smaller than the inverse lifetime of the state $\mathbf{k} + \mathbf{Q}$, i.e.

$|\varepsilon_{\mathbf{k}} - \varepsilon_{\mathbf{k}+\xi^{-1}}| < |\text{Im}\Sigma_{\mathbf{k}+\mathbf{Q}}|$. This can be fulfilled for a large ξ or for a band with large effective mass. Because of the small correlation length of our calculation, the shadow states can only be understood from the above discussed strong deformation of the quasi particle dispersion.

In the inset of Fig. 3, we show the frequency dependence of $\text{Im}\Sigma_{\mathbf{k}}(\omega)$ for various \mathbf{k} -points. We find a pronounced difference between momenta at the FS and away from it. At the FS, the transition from a low frequency ω^2 to a linear in ω behavior occurs below 0.005 eV. This extremely low energy scale is expected to be of importance for the anomalous transport properties of the high- T_c materials. At $\mathbf{k} = (\pi, \pi/8)$, where the shadow band crosses the Fermi level, we find a double well structure. This reflects the strong coupling of the shadow states to the main FS and is a precursor of the singular behavior of $\text{Im}\Sigma_{\mathbf{k}}(\omega)$ in the antiferromagnetic state [23]. This anomalous frequency dependence is different from the main assumption of the Luttinger theorem [22] ($\text{Im}\Sigma_{\mathbf{k}}(\omega) \propto \omega^2$) and leads to an occupation of shadow states and consequently to a violation of the theorem, shown in Fig. 1. An experimental indication for the violation of the Luttinger theorem in underdoped systems was recently found by Liu *et al.* [2].

In conclusion, we presented a new numerical method for the solution of the FLEX-equations on the real frequency axis, which permits the analysis of the fine structure of the excitation spectrum for high- T_c materials. A central role for all results shown here plays the exceptional behavior of the quasi particles at the X -point. The occurrence of a flat dispersion at the X -point was shown to be of extreme importance for a deep understanding of the shadows of the Fermi surface without broken antiferromagnetic order and for the violation of the Luttinger theorem. All this shows clearly that the quasiparticle properties of the high- T_c superconductors are closely intertwined with the strong antiferromagnetic fluctuations. In view of the importance of antiferromagnetic correlations for superconductivity [1], we extended our approach to the superconducting state, to investigate the phenomena discussed in this paper below T_c . [16]

¹ E. Dagotto, Rev. Mod. Phys. **66**, 763 (1994) and references therein.
² R. Liu, W. Veal, A.P. Paulikas, J. W. Downey, P. J. Kostić, S. Fleshler, U. Welp, C. G. Olson, X. Wu, A. J. Arko, and J. J. Joyce Phys. Rev. B **46**, 11056 (1992).
³ D. S. Dessau, Z.-X. Shen, D. M. King, D. S. Marshall, L. W. Lombardo, P. H. Dickinson, A. G. Loeser, J. DiCarlo,

C.-H. Park, A. Kapitulnik, and W. E. Spicer, Phys. Rev. Lett. **71**, 2781 (1993).
⁴ P. Aebi, J. Osterwalder, P. Schwaller, L. Schlappbach, M Shimoda, T. Mochiku, and K. Kadowaki, Phys. Rev. Lett. **72**, 2757 (1994).
⁵ K. Gofron, J. C. Campucano, A. A. Abrikosov, M. Lindroos, A. Bansil, H. Ding, D. Koelling, and B. Dabrowski, Phys. Rev. Lett. **73**, 3302 (1994).
⁶ B. O. Wells, Z.-X. Shen, A. Matsuura, D. M. King, M. A. Kastner, M. Greven, and R. J. Birgeneau, Phys. Rev. Lett. **74**, 964 (1995).
⁷ S. Chakravarty, Phys. Rev. Lett. **74**, 1885 (1995).
⁸ N. E. Bickers, D. J. Scalapino, Ann. Phys. (N.Y.) **193**, 206 (1989).
⁹ N. E. Bickers, D. J. Scalapino, and S. R. White, Phys. Rev. Lett. **62**, 961 (1989).
¹⁰ W. Serene and D. W. Hess, Phys. Rev. B **44**, 3391 (1991).
¹¹ T. Dahm and L. Tewordt, Phys. Rev. Lett **74**, 793 (1995).
¹² G. Baym and L. P. Kadanoff, Phys. Rev. **124**, 287 (1961); G. Baym *ibid.* **127**, 1391 (1962).
¹³ E. Dagotto, A. Nazarenko, and M. Bonisengi, Phys. Rev. Lett. **73**, 728 (1994).
¹⁴ N. Bulut, D.J. Scalapino, and S. R. White, Phys. Rev. Lett. **72**, 705 (1994).
¹⁵ R. Preuss, W. Hanke, and W. von der Linden, preprint.
¹⁶ S. Grabowski, J. Schmalian, M. Langer, and K.-H. Bennemann, unpublished.
¹⁷ A. A. Abrikosov, L. P. Gorkov, and I. Y. Dzyaloshinskii, *Quantum Field Theoretical Methods in Statistical Physics*, Pergamon Press, London (1965).
¹⁸ H. Schweitzer and G. Cycholl, Solid State Commun. **74**, 735 (1990).
¹⁹ Using FFT, one assumes the functions to be periodic in frequency. Consequently one has to chose the energy interval of the calculation in a way that $\Sigma_{\mathbf{k}}(\omega)$ is zero at the boundaries, fulfilled for $\omega \approx \pm 100t_o$, since it behaves like $1/\omega$ for large $|\omega|$. Therefore, we calculate the Laplace transform of $\Sigma_i(t) = \Sigma_i(t) - \Sigma_i(0) \exp\{-(t/\tau)^2\}$ with $\tau \approx 2t_o^{-1}$, which decreases faster than $1/\omega$ and the frequency range can be chosen much smaller ($\pm 30t_o$). The subtracted term can be transformed analytically.
²⁰ The calculations are performed on a (64×64) square lattice. We use 4096 equally spaced energy points in the interval $[-30t_o, 30t_o]$. In order to gain memory space, we skip most of these points by introducing a logarithmic mesh point scale after FFT, but keep the above point density in the low energy region. In order to perform a later FFT, the skipped points are recalculated by Padé interpolation, leading to a low energy resolution of $0.014t_o$.
²¹ H. Eskes, M. B. J. Meinders, and G. A. Sawatzky, Phys. Rev. Lett. **67**, 1035 (1991).
²² J. M. Luttinger, Phys. Rev. **119**, 1153 (1961).
²³ A. P. Kampf and J. R. Schrieffer, Phys. Rev. B **42**, 7967 (1990).
²⁴ J. M. Tranquada, P. M. Gehring, G. Shirane, S. Shamoto, and M. Sato, Phys. Rev. B **46**, 5561 (1992).